

Communication

A Cadmium Anionic 1-D Coordination Polymer $\{[\text{Cd}(\text{H}_2\text{O})_6][\text{Cd}_2(\text{atr})_2(\mu_2\text{-btc})_2(\text{H}_2\text{O})_4] 2\text{H}_2\text{O}\}_n$ within a 3-D Supramolecular Charge-Assisted Hydrogen-Bonded and π -Stacking Network

Anas Tahli^{1,2}, Ümit Köc¹, Reda F. M. Elshaarawy^{1,3}, Anna Christin Kautz¹ and Christoph Janiak^{1,*}

¹ Institut für Anorganische Chemie und Strukturchemie, Universitätsstr. 1, 40225 Düsseldorf, Germany; anas.tahli@gmx.de (A.T.); uemit.koec@gmail.com (Ü.K.); reda.elshaarawy@suezuniv.edu.eg (R.F.M.E.); Anna.Christin.Kautz@uni-duesseldorf.de (A.C.K.)

² Faculty of Science, Al-Furat University, Deir Ezzor, Syria

³ Faculty of Science, Suez University, 43533 Suez, Egypt

* Correspondence: janiak@hhu.de; Tel.: +49-211-81-12286

Academic Editor: Sławomir J. Grabowski

Received: 3 February 2016; Accepted: 26 February 2016; Published: 2 March 2016

Abstract: The hydrothermal reaction of 4,4'-bis(1,2,4-triazol-4-yl) (btr) and benzene-1,3,5-tricarboxylic acid (H_3btc) with $\text{Cd}(\text{OAc})_2 \cdot 2\text{H}_2\text{O}$ at 125 °C *in situ* forms 4-amino-1,2,4-triazole (atr) from btr, which crystallizes to a mixed-ligand, poly-anionic chain of $[\text{Cd}_2(\text{atr})_2(\mu_2\text{-btc})_2(\text{H}_2\text{O})_4]^{2-}$. Together with a hexaaquacadmium(II) cation and water molecules the anionic coordination-polymeric forms a 3-D supramolecular network of hexaaquacadmium(II)-*catena*-[bis(4-amino-1,2,4-triazole) tetraaquabis(benzene-1,3,5-tricarboxylato)dicadmiate(II)] dihydrate, 1-D- $\{[\text{Cd}(\text{H}_2\text{O})_6][\text{Cd}_2(\text{atr})_2(\mu_2\text{-btc})_2(\text{H}_2\text{O})_4] 2\text{H}_2\text{O}\}_n$ which is based on hydrogen bonds (in part charge-assisted) and π - π interactions.

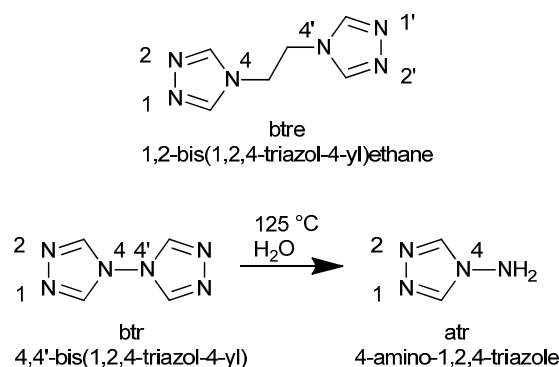
Keywords: hydrogen-bonded network; anionic coordination polymer; crystal engineering; charge-assisted H-bonds

1. Introduction

Metal-organic frameworks (MOFs) which are porous coordination polymers (PCPs) attract great interest for their potential applications in separation processes [1], sensor technology [2], luminescence [3], ionic or electrical conductivity [4,5], magnetism [6], and heat transformation through reversible water de- and adsorption [7,8]. Benzene carboxylic acid ligands, such as terephthalic acid or trimesic acid (H_3btc), are common rigid ligands for porous coordination polymers (PCPs). 1,2,4-Triazol-4-yl derivatives match the coordination geometry of pyrazoles with their N1 and N2 donor atoms, and can form different secondary building units (SBUs). The amino-functionalized triazole ligand 4-amino-1,2,4-triazole (atr) can coordinate to metal atoms to build molecular complexes [9,10], polynuclear complexes [11,12], inorganic-organic coordination polymers [13–16] and different dimensional metal-organic networks of mixed ligands [17,18].

Coordination polymers based on mixed-linkers allow for a fine-tuning of MOF properties and can show additional characteristics such as crystal-to-crystal transformations [19], short and long-range magnetic ordering [20], luminescence [21], *etc.* [22]. The combination of neutral nitrogen donor ligands with anionic carboxylate ligands are frequent choices for the synthesis of mixed-ligand networks [22]. The linker 1,2-bis(1,2,4-triazol-4-yl)ethane (abbreviated as btre, Scheme 1) has recently been intensely studied in mixed-linker MOFs [19–24] and single-linker networks [25]. Herein, we report an attempt

to construct a mixed-linker network with the 4,4'-bis(1,2,4-triazol-4-yl) (btr) ligand which was not hydrothermally stable under the synthesis conditions of 125 °C in water, so that the hydrolysis product 4-amino-1,2,4-triazole (atr) was incorporated instead (Scheme 1).



Scheme 1. Triazole ligands relevant in this work and indication of the hydrolysis of btr to atr.

2. Results and Discussion

Colorless crystals (Figure S1, Supplementary Information) were obtained from the hydrothermal reaction (125 °C) of $\text{Cd}(\text{OAc})_2 \cdot 2\text{H}_2\text{O}$, 4,4'-bis(1,2,4-triazol-4-yl) (btr) and benzene-1,3,5-tricarboxylic acid (H_3btc) in approximately 1:3:1 molar ratio in the presence of three equivalents of triethylamine as a base to deprotonate the carboxylate groups of H_3btc . The reaction was repeated several times and found reproducible. The crystals are soluble in water and ethanol.

Comparison between the FT-IR spectra (attenuated total reflection, ATR) of the crystalline product and the mixture of atr and H_3btc ligands (Figure S2, Supplementary Information) shows significant differences in the fingerprint region which suggests that the ligands became coordinated to the metal ion. Multiple weak broad peaks between 3300 and 3100 cm^{-1} can be assigned to the O–H/N–H stretching vibrations of aqua ligands and the amino group of the atr ligand [26]. The absence of a peak at ca 1715 cm^{-1} indicates the full deprotonation of the H_3btc ligand. Additionally, the asymmetric and symmetric stretching vibrations of the carboxylate group [27,28] are observed at 1607 cm^{-1} , 1204 cm^{-1} , and 1527 cm^{-1} , 1110 cm^{-1} , which reveal different binding modes of the carboxylate group. Bands at 752 cm^{-1} and 731 cm^{-1} in the fingerprint region are due to 1,3,5-trisubstituted benzene [27]. Furthermore, a band at 612 cm^{-1} can be assigned to the vibrational mode of the triazole ring of the atr ligand [29].

The sample was dissolved in DMSO-d_6 via heating in an ultrasonic bath at 50 °C. For the NMR analysis of the crystalline product an excess NaCN was added to the sample in order to bind the Cd^{2+} ions as stable cyanido complexes and to free the ligands so that a ligand ratio can be determined. After centrifugation, the pipette-separated supernatant was measured. The ^1H NMR spectrum (Figure S3, Supplementary Information) then shows both atr and btc ligand signals. The signal of the two protons of the triazole ring in the atr ligand appears at 9.17 ppm and the signal for the (protonated) amino group is observed at 6.30 ppm. The signal at 8.36 is assigned to the three protons of the btc benzene ring. Signals for residual Et_3N appeared at ~0.89–0.92 and ~2.37–2.42 ppm. The integration ratio between atr: btc and NH_3^+ is 1.0:1.7:1.7 which agrees with two H-atoms for the triazole ring, three H-atoms of btc (1:1.5) and three H-atoms for the protonated amino group (1:1.5).

The title compound crystallizes in the monoclinic crystal system with the $P2_1/c$ space group. The crystallographic asymmetric unit (Figure 1a) consists of a Cd(II) ion with benzene-tricarboxylate (btc^{3-}), 4-amino-1,2,4-triazole (atr), and two aqua ligands, plus a half-occupied cationic hexaaquacadmium(II) complex and a lattice water molecule. The original precursor compound 4,4'-bis(1,2,4-triazol-4-yl) (btr) is not incorporated as a ligand into the structure due to the *in situ* hydrolysis into 4-amino-1,2,4-triazole (atr), which was then found instead. Yet, the slow delivery of atr in the course of the reaction is apparently crucial for the product formation. When the reaction was carried out with atr directly instead of btr no crystals or precipitate formed. The charge-neutral product formula is 1-D $[\{\text{Cd}(\text{H}_2\text{O})_6\}][\text{Cd}_2(\text{atr})_2(\mu_2\text{-btc})_2(\text{H}_2\text{O})_4] 2\text{H}_2\text{O}]_n$, **1**, named hexaaqua-cadmium(II)-catena-[bis(4-amino-1,2,4-triazole)tetraaquabis(benzene-1,3,5-tricarboxylato) dicadmate(II)] dihydrate.

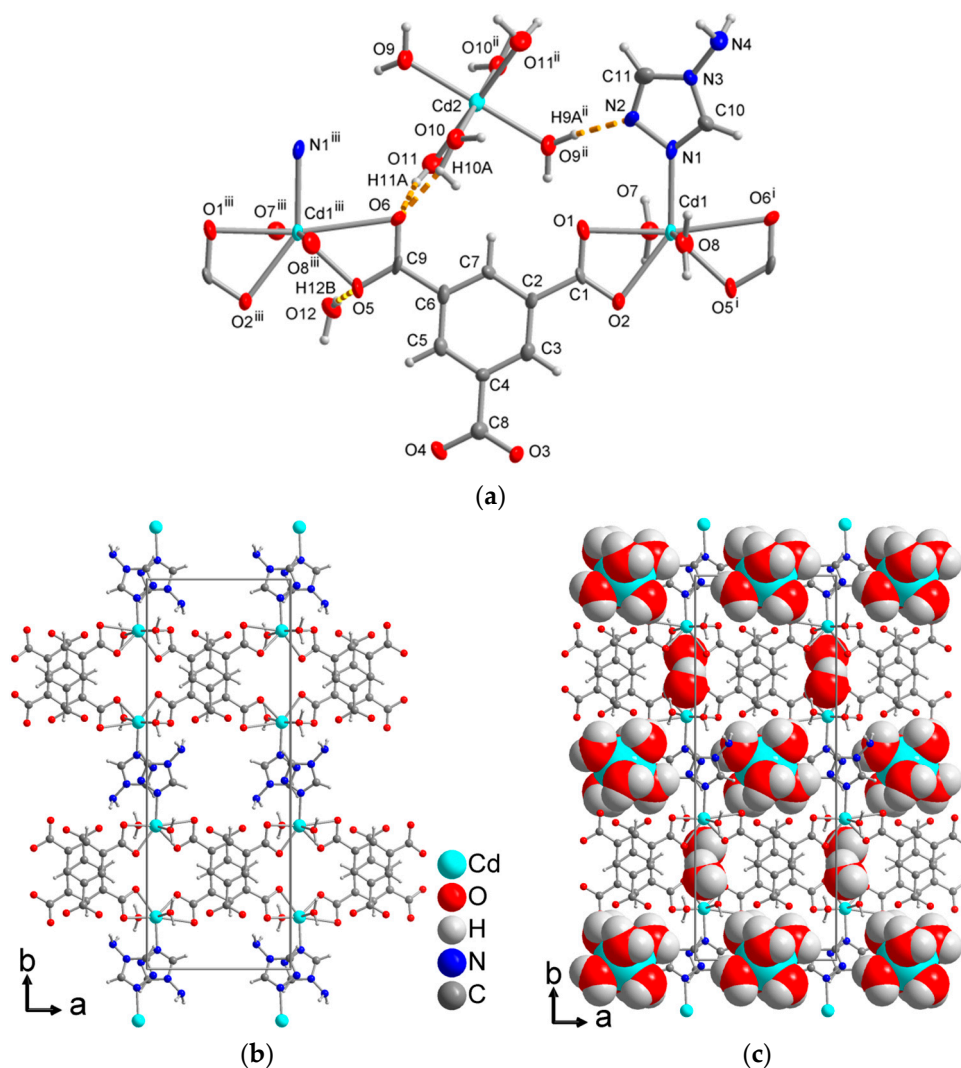


Figure 1. (a) Extended asymmetric unit of **1** (70% thermal ellipsoids, hydrogen atoms with arbitrary radii), showing also part of the hydrogen bonds (orange dashed lines). Symmetry transformations $i = x + 1, y, z$; $ii = -x + 1, -y + 1, -z + 1$; $iii = x - 1, y, z$. Section of the packing diagram of (b) the anionic chains and (c) the full structure with the $[\text{Cd}(\text{H}_2\text{O})_6]^{2+}$ cations and the crystal water molecules highlighted in space-filling mode. Selected distances and angles are given in Table 1 and details of H-bonds in Table 2.

Table 1. Selected bond lengths [Å] and angles [°] in **1**.

Cd1–N1	2.253(6)	O8–Cd1–O7	171.88(16)
Cd1–O1	2.412(5)	N1–Cd1–O2	142.95(16)
Cd1–O2	2.355(5)	O5 ⁱ –Cd1–O2	84.36(16)
Cd1–O5 ⁱ	2.258(5)	O8–Cd1–O2	89.48(18)
Cd1–O6 ⁱ	2.766(5)	O7–Cd1–O2	82.40(17)
Cd1–O7	2.325(5)	N1–Cd1–O1	88.09(17)
Cd1–O8	2.302(5)	O5 ⁱ –Cd1–O1	139.22(16)
–	–	O8–Cd1–O1	90.35(17)
Cd2–O9	2.275(5)	O7–Cd1–O1	84.81(17)
Cd2–O10	2.304(6)	O2–Cd1–O1	54.86(15)
Cd2–O11	2.266(5)	–	–
–	–	O9–Cd2–O10	86.65(18)
N1–Cd1–O5 ⁱ	132.67(18)	O9–Cd2–O10 ⁱⁱ	93.35(18)
N1–Cd1–O8	90.45(19)	O10–Cd2–O11	86.1(2)
O5 ⁱ –Cd1–O8	88.47(18)	O10–Cd2–O11 ⁱⁱ	93.9(2)
N1–Cd1–O7	95.88(18)	O9–Cd2–O11	87.50(19)
O5 ⁱ –Cd1–O7	90.94(17)	O9–Cd2–O11 ⁱⁱ	92.50(19)

Symmetry transformations used to generate equivalent atoms: $i = x + 1, y, z$; $ii = -x + 1, -y + 1, -z + 1$.

Table 2. Details of the hydrogen bonding interactions in **1**^a.

D–H...A	D–H [Å]	H...A [Å]	D...A [Å]	D–H...A [°]	Symmetry Transformations
O7–H7A...N3 ^{iv}	0.95	2.33	3.280(7)	176	$iv = -x + 2, -y + 1, -z + 1$
O7–H7A...N4 ^{iv}	0.95	2.33	3.138(8)	143	$iv = -x + 2, -y + 1, -z + 1$
O7–H7B...O12 ⁱ	0.95	2.07	2.684(7)	121	$i = x + 1, y, z$
O8–H8A...O11 ^v	0.95	2.41	3.284(7)	152	$v = x + 1, y, z + 1$
O8–H8B...O12 ^v	0.95	2.05	2.695(7)	124	$v = x + 1, y, z + 1$
O9–H9A...O3 ^{vi}	0.92(4)	1.88(5)	2.785(7)	167(8)	$vi = -x + 1, y + 1/2, -z + 3/2$
O9–H9B...N2 ⁱⁱ	0.89(9)	2.02(9)	2.897(8)	171(8)	$ii = -x + 1, -y + 1, -z + 1$
O10–H10A...O6	0.95(9)	1.84(9)	2.742(7)	158(7)	–
O10–H10B...N4 ^{vii}	0.98(5)	1.91(6)	2.803(8)	151(7)	$vii = -x + 2, -y + 1, -z + 2$
O11–H11A...O6	1.00(9)	1.93(9)	2.906(8)	167(8)	–
O11–H11B...O4 ^{viii}	0.92(5)	1.78(6)	2.641(7)	155(8)	$viii = x, -y + 1/2, z - 1/2$
O12–H12A...O2 ^x	0.89(5)	1.84(6)	2.661(7)	152(8)	$x = x - 1, -y + 1/2, z - 1/2$
O12–H12B...O5	0.92	1.85	2.763(7)	172	–
N4–H4A...O3 ^{ix}	0.85(8)	2.24(8)	3.081(8)	170(7)	$ix = 2 - x, y + 1/2, -z + 3/2$
N4–H4B...O1 ^{vii}	0.83(4)	2.04(5)	2.857(8)	166(8)	$vii = -x + 2, -y + 1, -z + 2$
C10–H10...O10 ⁱ	0.95	2.54	3.381(8)	147	$i = x + 1, y, z$

Notes: ^a D = donor, A = acceptor.

The Cd1 ion forms a coordination polymeric chain with benzene-tricarboxylate (btc^{3-}), 4-amino-1,2,4-triazole (atr), and two aqua ligands. The Cd1 atom is seven-fold coordinated in a distorted pentagonal-bipyramidal fashion by a triazole nitrogen atom of atr and six oxygen atoms; two of them belong to axial aqua ligands. The other four O-atoms come from the carboxylate groups of two fully deprotonated btc^{3-} ligands, which coordinate in a bidentate chelating mode. The O-atoms of btc^{3-} and the N-atom of atr form the equatorial plane of the pentagonal bipyramid. One of these chelated Cd–O bonds is slightly longer (Cd1–O6 = 2.766(5) Å) than the range of the other Cd–O bonds (Cd1–O = 2.258(5)–2.412(5) Å). The atr ligand coordinates to Cd1 through the imine N1-atom of the triazole ring as a terminal ligand; the other imine N atom (N2) and the amino group remain without Cd coordination but engage in hydrogen bonding (see below). The tri-anionic btc^{3-} ligands coordinate as bridges between two Cd1 atoms to form the one-dimensional mixed-ligand chain (Figure 1b); the third

carboxylate group remains uncoordinated but is part of the hydrogen-bonding network. This chain is a polyanion and has the formula of $[\text{Cd}_2(\text{atr})_2(\mu_2\text{-btc})_2(\text{H}_2\text{O})_4]_n^{2-}$. Charge neutrality is reached by one hexaaquacadmium(II) cation, $[\text{Cd}(\text{H}_2\text{O})_6]^{2+}$ as equivalent for each of the two Cd1 atoms. The Cd2 atom in $[\text{Cd}(\text{H}_2\text{O})_6]^{2+}$ sits on an inversion center as a special position (Figure 1a). Hexa-coordinated cadmium can have a coordination environment in-between octahedral and trigonal prismatic [30,31]. Here, the Cd2 atom has a slightly distorted octahedral environment of six water molecules. Two crystal water molecules per formula unit of 1-D $[\text{Cd}(\text{H}_2\text{O})_6][\text{Cd}_2(\text{atr})_2(\mu_2\text{-btc})_2(\text{H}_2\text{O})_4] 2\text{H}_2\text{O}$ complete the packing (Figure 1c).

Anionic coordination polymers are not very frequent in view of the several thousand publications on coordination polymers [32]. Only a few of the ones which are reported feature the metal cadmium, as in $[\text{Cd}(\text{P}_6\text{O}_{18})(\text{H}_2\text{O})_2]^{2-}$ [33], $[\text{Cd}(\text{OABDC})(\text{H}_2\text{O})_2]^- \cdot (\text{OABDC} = 5\text{-}(\text{carboxylatomethoxy})\text{benzene-1,3-dicarboxylato})$ [34], and in $[\text{Cd}(\text{P}_6\text{O}_{18})]_n^{4-}$ [35].

The infinite anionic chains are stacked parallel to each other along the *c* direction (Figure 1b) through significant π - π interactions [36] between the adjacent benzene rings of the btc^{3-} ligands and the adjacent triazole rings of the atr ligands, respectively (Figure 2a). Strong π -stacking interactions have rather short centroid-centroid contacts ($<3.8 \text{ \AA}$) and near parallel ring planes which translate into a sizable overlap of the aryl-plane areas. The centroid-centroid distance of adjacent btc -benzene rings is $3.726(4) \text{ \AA}$ and for neighboring triazole rings it is $3.598(4)$ and $3.997(4) \text{ \AA}$ (Figure 2a). The interplanar angle of the benzene rings is 4° ; the triazole rings are exactly parallel by symmetry; (see Supplementary Information for further details, Scheme S1 and Table S1). In addition to π -stacking the inter-chain packing is controlled by charge-assisted amino-N-H \cdots $(^-)\text{O}_2\text{C}$ -hydrogen bonds ($\text{N4-H} \cdots \text{O1}$ and O3 , Figure 2b and Table 2). The carboxylate groups of btc^{3-} as hydrogen bond acceptors carry negative ionic charges. Such charge-assisted H-bonds are usually stronger and shorter than neutral H-bonds [37–42].

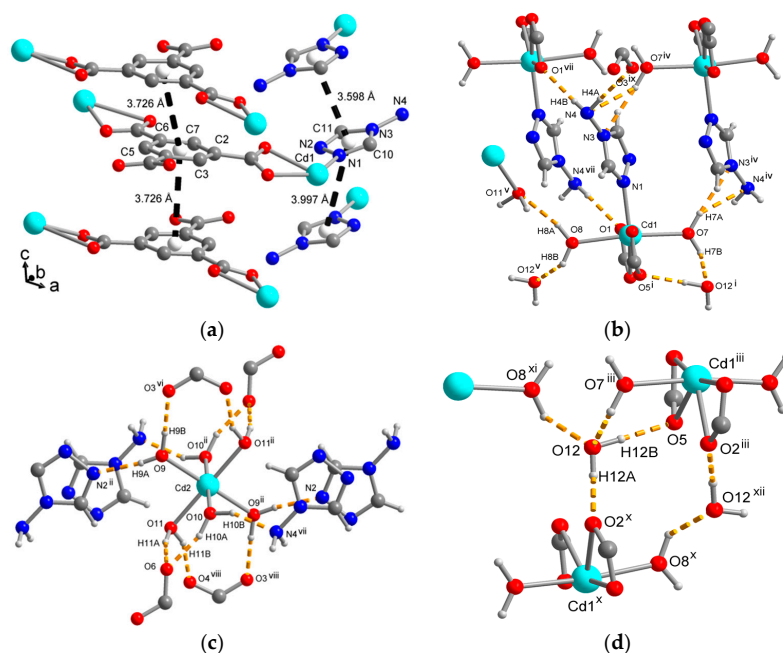


Figure 2. Supramolecular packing interactions in 1: (a) π -stacking interactions with centroid-centroid contacts given. Hydrogen-bonding interactions shown separately for the different H-bond donors for clarity: (b) around the $[\text{Cd}(\text{H}_2\text{O})_6]^{2+}$ cations, (c) around the 4-amino-1,2,4-triazole (atr) ligands, and (d) around the crystal water molecule. Details of π -stacking interactions are given in Supplementary Information, details of H-bonds together with symmetry transformations are listed in Table 2. Additional symmetry transformations used in (d): $iii = x - 1, y, z$; $xi = x - 1, y, z - 1$; $xii = x, -y + 1/2, z + 1/2$.

The space which is created between the parallel anion chains is occupied by the cationic $[\text{Cd}(\text{H}_2\text{O})_6]^{2+}$ complexes and lattice water molecules (Figure 1c). Both $[\text{Cd}(\text{H}_2\text{O})_6]^{2+}$ and the crystal water molecules function as H-bond donors towards the carboxylate oxygen atoms, again with charge-assisted $\text{O}-\text{H} \cdots (^-)\text{O}_2\text{C}-$ hydrogen bonds (Figure 2c,d). The O9 atom of $[\text{Cd}(\text{H}_2\text{O})_6]^{2+}$ also forms a hydrogen bond towards the N2-triazole atom (Figure 2c). The crystal water oxygen atom O12 and O11 of $[\text{Cd}(\text{H}_2\text{O})_6]^{2+}$ act further as H-bond acceptors from the aqua ligands (O7, O8) on Cd1 in the anionic chain (Figure 2b,d). Overall this gives a tight hydrogen bonding network which, apparently, prevents any disorder in the crystal water and allowed for the finding and refining of most protic H-atom positions (see X-ray crystallography section).

Together, the π - π interactions between adjacent anionic chains and the hydrogen bonds between cationic complexes and anionic chains and lattice water molecules build a 3-D supramolecular network (Figure 1c).

3. Materials and Methods

Reagents and solvents were obtained from commercial sources and used without any further purification. The bis(1,2,4-triazol-4-yl) ligand (btr) was synthesized under inert conditions according to previous work [43] from hydrazine monohydrate, $\text{N}_2\text{H}_4 \cdot \text{H}_2\text{O}$, N,N' -dimethylformamide azine [44], and *p*-toluenesulfonic acid monohydrate in dry toluene. A programmable oven type (UFP 400) from Memmert GmbH (Schwabach, Germany) was used for the hydrothermal synthesis. The reactions were carried out in DURAN[®] (DURAN Group GmbH, Wertheim, Germany) culture glass tubes with PTFE-faced sealing wad, diameter 12 mm, height 100 mm, and DIN thread 14 GL, closed with a red screw cap (Figure S4, Supplementary Information), suitable for hydro-/solvothermal synthesis for coordination polymer synthesis up to 150 °C instead of an autoclave. The contents only come into contact with the glass and polytetrafluoroethylene (PTFE) seal. Elemental analyses were performed on a Vario MicroCube from Elementar GmbH. The light microscopy images were observed with a Leica MS5 binocular eyepiece with transmitted light and polarization filter. The images of isolated crystals were taken with a Nikon COOLPIX 4500 (Tokyo, Japan) digital camera through a special ocular connection. Infrared spectra were recorded with a Bruker Optik TENSOR 37 spectrophotometer (Bruker Optik GmbH, Ettlingen, Germany) using a Diamond ATR (Attenuated Total Reflection) unit from 4000 to 500 cm^{-1} . The following abbreviations were used to classify spectral bands: br (broad), sh (shoulder), vw (very weak), w (weak), m (medium), s (strong), and vs (very strong). The ¹H-NMR spectra were recorded on a Bruker Advance DRX 500 MHz NMR spectrometer with calibration against the residual protonated solvent signal DMSO-*d*₆ (2.50 ppm).

1D $\{[\text{Cd}(\text{H}_2\text{O})_6][\text{Cd}_2(\text{atr})_2(\mu_2\text{-btc})_2(\text{H}_2\text{O})_4] \cdot 2\text{H}_2\text{O}\}_n$: A portion of $\text{Cd}(\text{OAc})_2 \cdot 2\text{H}_2\text{O}$ (10.7 mg, 0.04 mmol) and 4,4'-bis(1,2,4-triazol-4-yl) (btr) (16.3 mg, 0.12 mmol) was combined in 1 mL of water in a DURAN glass tube and shaken for about 3 min. Then a solution of benzene-1,3,5-tricarboxylic acid (H_3btc) (8.4 mg, 0.04 mmol) and $\text{Et}_3\text{N}/\text{H}_2\text{O}$ (0.75 mL of 0.16 mol/L, 3eq. to H_3btc) in 2.5 mL of water prepared in an ultrasonic bath at 45–50 °C was added to the previous mixture. The sealed glass tube was shaken for about 5 min and then placed in a programmable furnace, heated to 125 °C for 3 h and held at that temperature for 48 h, then cooled at a rate of 5 °C/h to ambient temperature. The resulting colorless crystals were separated from powdery precipitate and washed with the mother liquor. Yield: (14 mg, 30% based on metal salt). FT-IR (ATR, cm^{-1}): 3100 (w, ν (C–H)), 1607 (s, ν_{asym} C=O, C=N), 1527 (m, ν_{sym} C=O, C=N), 1204 (s, ν_{asym} C–O, C–N), 1110 (s, ν_{sym} C–O, C–N), 871 (m, sh, γ (C–H)), 752, 731 (s, γ , 1,3,5-trisubstituted benzene ring of Hbtc), 612 (m, γ , triazole ring). Calcd. for $\text{C}_{22}\text{H}_{38}\text{Cd}_3\text{N}_8\text{O}_{24}$ ($M_w = 1135.8 \text{ g mol}^{-1}$): C 23.27, H 3.37, N 9.87; found: C 23.35, H 2.99, N 10.35%.

Single Crystal X-Ray Structure

A suitable single crystal (Figure S1, Supplementary Information) was carefully selected under a polarizing microscope and mounted in oil in a glass loop. Data collection: Bruker AXS APEX II CCD area-detector diffractometer with multilayer mirror monochromator, Mo-K α radiation ($\lambda = 0.71073 \text{ \AA}$)

from microsource, double-pass method with φ - and ω -scans; data collection with APEX2, cell refinement and data reduction with SAINT [45], experimental absorption correction with SADABS [46]. Structure analysis and refinement: All structures were solved by direct methods using SHELXL2014; refinement was done by full-matrix least squares on F^2 using the SHELX-97 program suite [47]. Non-hydrogen atoms were refined with anisotropic displacement parameters. All non-hydrogen positions were found and refined with anisotropic temperature factors. Hydrogen atoms for aromatic CH were positioned geometrically (CH = 0.95 Å) and refined using a riding model (AFIX 43) with $U_{\text{iso}}(\text{H}) = 1.2U_{\text{eq}}(\text{C})$. Hydrogen atoms on aqua ligands and on the amino, NH₂ group were treated in a mixed refinement. On O7 and O8 the H atoms were positioned geometrically (O–H = 0.95 Å, N–H = 0.88 Å) and refined using a riding model (AFIX 93) with $U_{\text{iso}}(\text{H}) = 1.5U_{\text{eq}}(\text{O},\text{N})$. On O9, O10, O11, O12 and N4 the H atoms could be found and refined with $U_{\text{iso}}(\text{H}) = 1.5U_{\text{eq}}(\text{O},\text{N})$ and DFIX constraints (0.95, 0.05) for H9B, O10B, H11B, N4B, and O12A. H12B was found but had to be kept fixed upon further refinement (AFIX 1). The two highest peaks in the electron density map are within 1.52 Å of the Cd1 atom, the next two highest peaks are within 1.5 Å of Cd2. Details of the X-ray crystal data structure determination and refinement are provided in Table 3. Graphics were drawn with DIAMOND (Version 3.2) [48] Analyses on the supramolecular π – π -stacking interactions were done with PLATON for Windows [49]. CCDC No. 1451376 contains the supplementary crystallographic data for this paper. These data can be obtained free of charge via <http://www.ccdc.cam.ac.uk/conts/retrieving.html>.

Table 3. Crystal data and refinement details for 1-D $[\text{Cd}(\text{H}_2\text{O})_6][\text{Cd}_2(\text{atr})_2(\mu_2\text{-btc})_2(\text{H}_2\text{O})_4] \cdot 2\text{H}_2\text{O}]_n$, **1**.

Chemical Formula	$\text{C}_{22}\text{H}_{38}\text{Cd}_3\text{N}_8\text{O}_{24}$
Mr	1131.80
Crystal system, space group	Monoclinic, $P 2_1/c$
Temperature (K)	100(2)
a (Å)	10.1435(18)
b (Å)	26.471(5)
c (Å)	7.0263(13)
β (°)	106.213(13)
V (Å ³)	1811.6(6)
Z	2
Density (calculated), Mg/m ³	2.082
Absorpt. coefficient, μ (mm ^{−1})	1.850
Crystal size (mm)	0.3 × 0.3 × 0.1
$F(000)$	1124
Theta range for data collection, (°)	2.09–25.34
h, k, l ranges	±12, ±31, ±8
Reflections collected	15909
Independent reflections	3279 [$R(\text{int}) = 0.1114$]
Completeness to theta 25.34°	98.9%
Data/restraints/parameters	3279/5/286
Final R indices [$I > 2\sigma(I)$] ^a	$R1 = 0.0519, wR2 = 0.1284$
R indices (all data) ^a	$R1 = 0.0734, wR2 = 0.1418$
Goodness-of-fit on F^2 ^b	1.020
Weighting scheme $w; a/b$ ^c	0.0521/0.000
$\Delta\rho_{\text{max}}, \Delta\rho_{\text{min}}$ (e Å ^{−3}) ^d	0.30, −0.34

^a $R_1 = [\sum(|F_o| - |F_c|)] / \sum |F_o|$; $wR_2 = [\sum[w(F_o^2 - F_c^2)^2] / \sum[w(F_o^2)^2]]^{1/2}$; ^b Goodness-of-fit, $S = [\sum[w(F_o^2 - F_c^2)^2] / (n-p)]^{1/2}$; ^c $w = 1 / [\sigma^2(F_o^2) + (aP)^2 + bP]$ where $P = (\max(F_o^2 \text{ or } 0) + 2F_c^2) / 3$; ^d Largest difference peak and hole.

Supplementary Materials: The supplementary files are available online at <http://www.mdpi.com/2073-4352/6/3/23/s001>.

Acknowledgments: Anas Tahli sincerely thanks the Al-Furat University and the Ministry of Higher Education in Syria for the financial support (scholarship) during his study in Germany (language course, Master and PhD degree). The work was supported by the German Science Foundation (DFG) through grant Ja466/25-1.

Author Contributions: Anas Tahli and Ümit Köc designed the experiments, synthesized the btr ligand and compound **1**. X-ray measurements by Anna Christin Kautz, data analysis by Anas Tahli. Anas Tahli, Reda Elshaarawy and Christoph Janiak have written the manuscript.

Conflicts of Interest: The authors declare no conflict of interest.

References

1. Li, J.-R.; Sculley, J.; Zhou, H.-C. Metal–Organic Frameworks for Separations. *Chem. Rev.* **2012**, *112*, 869–932. [[CrossRef](#)] [[PubMed](#)]
2. Hu, Z.; Deibert, B.J.; Li, J. Luminescent metal–organic frameworks for chemical sensing and explosive detection. *Chem. Soc. Rev.* **2014**, *43*, 5815–5840. [[CrossRef](#)] [[PubMed](#)]
3. Cui, Y.-J.; Yue, Y.-F.; Qian, G.-D.; Chen, B.-L. Luminescent Functional Metal–Organic Frameworks. *Chem. Rev.* **2012**, *112*, 1126–1162. [[CrossRef](#)] [[PubMed](#)]
4. Horike, S.; Umeyama, D.; Kitagawa, S. Ion Conductivity and Transport by Porous Coordination Polymers and Metal–Organic Frameworks. *Acc. Chem. Res.* **2013**, *46*, 2376–2384. [[CrossRef](#)] [[PubMed](#)]
5. Givajva, G.; Amo-Ochoa, P.; Gómez-García, C.J.; Zamora, F. Electrical conductive coordination polymers. *Chem. Soc. Rev.* **2012**, *41*, 115–147. [[CrossRef](#)] [[PubMed](#)]
6. Kurmoo, M. Magnetic metal–organic frameworks. *Chem. Soc. Rev.* **2009**, *38*, 1353–1379. [[CrossRef](#)] [[PubMed](#)]
7. Fröhlich, D.; Henninger, S.K.; Janiak, C. Multicycle water vapour stability of microporous breathing MOF aluminium isophthalate CAU-10-H. *Dalton Trans.* **2014**, *43*, 15300–15304. [[CrossRef](#)] [[PubMed](#)]
8. Jeremias, F.; Fröhlich, D.; Janiak, C.; Henninger, S.K. Water and methanol adsorption on MOFs for fast cycling heat transformation processes. *New J. Chem.* **2014**, *38*, 1846–1852. [[CrossRef](#)]
9. Wang, S.-W.; Yang, L.; Feng, J.-L.; Wu, B.-D.; Zhang, J.-G.; Zhang, T.-L.; Zhou, Z.-N. Synthesis, Crystal Structure, Thermal Decomposition, and Sensitive Properties of Two Novel Energetic Cadmium(II) Complexes Based on 4-Amino-1,2,4-triazole. *Z. Anorg. Allg. Chem.* **2011**, *637*, 2215–2222. [[CrossRef](#)]
10. Carpenter, J.A.; Dshemuchadse, J.; Busato, S.; Braeunlich, I.; Pöthig, A.; Caseri, W. Tetrakis(4-amino-1,2,4-triazole)platinum(II) Salts: Syntheses, Crystal Structures, and Properties. *Z. Anorg. Allg. Chem.* **2014**, *640*, 724–732. [[CrossRef](#)]
11. Zhou, J.-H.; Cheng, R.-M.; Song, Y.; Li, Y.-Z.; Yu, Z.; Chen, X.-T.; Xue, Z.-L.; You, X.-Z. Syntheses, Structures, and Magnetic Properties of Unusual Nonlinear Polynuclear Copper(II) Complexes Containing Derivatives of 1,2,4-Triazole and Pivalate Ligands. *Inorg. Chem.* **2005**, *44*, 8011–8022. [[CrossRef](#)] [[PubMed](#)]
12. Yoo, H.-S.; Lim, J.-H.; Kang, J.-S.; Koh, E.-K.; Hong, C.-S. Triazole-bridged magnetic M(II) assemblies (M = Co, Ni) capped with the end-on terephthalate dianion involving multi-intermolecular contacts. *Polyhedron* **2007**, *26*, 4383–4388. [[CrossRef](#)]
13. Yeh, C.-W.; Chang, W.-J.; Suen, M.-C.; Lee, H.-T.; Tsai, H.-A.; Tsou, C.-H. Roles of the anion in the self-assembly of silver(I) complexes containing 4-amino-1,2,4-triazole. *Polyhedron* **2013**, *61*, 151–160. [[CrossRef](#)]
14. Wu, X.-Y.; Kuang, X.-F.; Zhao, Z.-G.; Chen, S.-C.; Xie, Y.-M.; Yu, R.-M.; Lu, C.-Z. A series of POM-based hybrid materials with different copper/aminotriazole motifs. *Inorg. Chim. Acta* **2010**, *363*, 1236–1242. [[CrossRef](#)]
15. Grosjean, A.; Daro, N.; Kaufmann, B.; Kaiba, A.; Létard, J.-F.; Guionneau, P. The 1-D polymeric structure of the [Fe(NH₂trz)](NO)₂·nH₂O (with n = 2) spin crossover compound proven by single crystal investigations. *Chem. Commun.* **2011**, *47*, 12382–12384. [[CrossRef](#)] [[PubMed](#)]
16. Gou, Y.-T.; Yue, F.; Chen, H.-M.; Liu, G.; Sun, D.-C. Syntheses and structures of 3d–4d heterometallic coordination polymers based on 4-amino-1,2,4-triazole. *J. Coord. Chem.* **2013**, *66*, 1889–1896. [[CrossRef](#)]
17. Yang, E.-C.; Zhang, C.-H.; Liu, Z.-Y.; Zhang, N.; Zhao, L.-N.; Zhao, X.-J. Three copper(II) 4-amino-1,2,4-triazole complexes containing differently deprotonated forms of 1,3,5-benzenetricarboxylic acid: Synthesis, structures and magnetism. *Polyhedron* **2012**, *40*, 65–71. [[CrossRef](#)]
18. Wang, X.-L.; Zhao, W.; Zhang, J.-W.; Lu, Q.-L. Three tetranuclear copper(II) cluster-based complexes constructed from 4-amino-1,2,4-triazole and different aromatic carboxylates: Assembly, structures, electrochemical and magnetic properties. *J. Solid State Chem.* **2013**, *198*, 162–168. [[CrossRef](#)]

19. Habib, H.A.; Sanchiz, J.; Janiak, C. Mixed-ligand coordination polymers from 1,2-bis(1,2,4-triazol-4-yl)-ethane and benzene-1,3,5-tricarboxylate: Trinuclear nickel or zinc secondary building units for three dimensional networks with crystal-to-crystal transformation upon dehydration. *Dalton Trans.* **2008**, 1734–1744. [[CrossRef](#)] [[PubMed](#)]
20. Habib, H.A.; Sanchiz, J.; Janiak, C. Magnetic and luminescence properties of Cu(II), Cu(II)₄O₄ core, and Cd(II) mixed-ligand metal–organic frameworks constructed from 1,2-bis(1,2,4-triazol-4-yl)ethane and benzene-1,3,5-tricarboxylate. *Inorg. Chim. Acta* **2009**, *362*, 2452–2460. [[CrossRef](#)]
21. Habib, H.A.; Hoffmann, A.; Höpfe, H.A.; Janiak, C. Crystal structures and solid-state CPMAS ¹³C NMR correlations in luminescent zinc(II) and cadmium(II) mixed-ligand coordination polymers constructed from 1,2-bis(1,2,4-triazol-4-yl)ethane and benzenedicarboxylate. *Dalton Trans.* **2009**, 1742–1751. [[CrossRef](#)] [[PubMed](#)]
22. Yin, Z.; Zhou, Y.-L.; Zeng, M.-H.; Kurmoo, M. The concept of mixed organic ligands in metal–organic frameworks: design, tuning and functions. *Dalton Trans.* **2015**, *44*, 5258–5275. [[CrossRef](#)] [[PubMed](#)]
23. Ding, J.-G.; Zhu, X.; Cui, Y.-F.; Liang, N.; Sun, P.-P.; Chen, Q.; Li, B.-L.; Li, H.-Y. Structurally versatile cadmium coordination polymers based on bis(1,2,4-triazol)ethane and rigid aromatic multicarboxylates: Syntheses, structures and properties. *CrystEngComm* **2014**, *16*, 1632–1644. [[CrossRef](#)]
24. Habib, H.A.; Janiak, C. Benzene-1,3,5-tricarboxylic acid-1,2-bis-(1,2,4-triazol-4-yl)ethane-water (4/1/2). *Acta Crystallogr. Sect. E Struct. Rep. Online* **2008**, *64*, o1199. [[CrossRef](#)] [[PubMed](#)]
25. Habib, H.A.; Hoffmann, A.; Höpfe, H.A.; Steinfeld, G.; Janiak, C. Crystal Structure Solid-State Cross Polarization Magic Angle Spinning ¹³C NMR Correlation in Luminescent d¹⁰ Metal-Organic Frameworks Constructed with the 1,2-Bis(1,2,4-triazol-4-yl)ethane Ligand. *Inorg. Chem.* **2009**, *48*, 2166–2180. [[CrossRef](#)] [[PubMed](#)]
26. Nakamoto, K. *Infrared and Raman Spectra of Inorganic and Coordination Compounds*; Wiley: New York, NY, USA, 1970.
27. Shi, Z.; Li, G.; Wang, L.; Gao, L.; Chen, X.; Hua, J.; Feng, S. Two Three-Dimensional Metal–Organic Frameworks from Secondary Building Units of Zn₈(OH)₄(O₂C–)₁₂ and Zn₂((OH)(O₂C–)₃: [Zn₂(OH)(btc)]₂(4,4'-bipy) and Zn₂(OH)(btc)(pipe). *Cryst. Growth Des.* **2004**, *4*, 25–27. [[CrossRef](#)]
28. Dai, J.-C.; Wu, X.-T.; Fu, Z.-Y.; Cui, C.-P.; Hu, S.-M.; Du, W.-X.; Wu, L.-M.; Zhang, H.-H.; Sun, R.-Q. Synthesis, Structure, and Fluorescence of the Novel Cadmium(II)–Trimesate Coordination Polymers with Different Coordination Architectures. *Inorg. Chem.* **2002**, *41*, 1391–1396. [[CrossRef](#)] [[PubMed](#)]
29. Slangen, P.M.; van Koningsbruggen, P.J.; Goubitz, K.; Haasnoot, J.G.; Reedijk, J. Isotropic Magnetic Exchange Interaction through Double μ-1,2,4-Triazolato-N₁,N₂ Bridges: X-ray Crystal Structure, Magnetic Properties, and EPR Study of Bis(μ-3-pyridin-2-yl-1,2,4-triazolato-N',N₁,N₂)(sulfato-O)aquacopper(II)-diaquacopper(II) Trihydrate. *Inorg. Chem.* **1994**, *33*, 1121–1126. [[CrossRef](#)]
30. Stiefel, E.I.; Brown, G.F. Detailed nature of the six-coordinate polyhedra in tris(bidentate ligand) complexes. *Inorg. Chem.* **1972**, *11*, 434–436. [[CrossRef](#)]
31. Banerjee, S.; Ghosh, A.; Wu, B.; Lassahn, P.-G.; Janiak, C. Polymethylene spacer regulated structural divergence in cadmium complexes: Unusual trigonal prismatic and severely distorted octahedral coordination. *Polyhedron* **2005**, *24*, 593–599. [[CrossRef](#)]
32. Janiak, C.; Vieth, J.K. MOFs, MILs and more: Concepts, properties and applications for porous coordination networks (PCNs). *New J. Chem.* **2010**, *34*, 2366–2388. [[CrossRef](#)]
33. Ameer, I.; Dkhili, S.; Sbihi, H.; Besbes-Hentati, S.; Rzaigui, M.; Abid, S. A Cadmium Coordination Polymer Based on Phosphate Clusters: Synthesis, Crystal Structure, Electrochemical Investigation and Antibacterial Activity. *J. Cluster Sci.* **2016**. [[CrossRef](#)]
34. Wang, P.; Zhao, Y.; Chen, Y.; Kou, X.-Y. A novel one-dimensional tubular cadmium(II) coordination polymer based on 5-(carboxylatomethoxy)benzene-1,3-dicarboxylate containing 4-aminopyridinium ions. *Acta Crystallogr. Sect. C Cryst. Struct. Commun.* **2013**, *69*, 1340–1343. [[CrossRef](#)] [[PubMed](#)]
35. Abid, S.; Al-Deyab, S.S.; Rzaigui, M. The one-dimensional coordination polymer poly[tetrakis [(4-chloro-phenyl)methanaminium] [cadmate-μ-cyclohexaphosphorato]]. *Acta Crystallogr. Sect. E Struct. Rep. Online* **2011**, *67*, m1549–m1550. [[CrossRef](#)] [[PubMed](#)]
36. Janiak, C. A critical account on π–π stacking in metal complexes with aromatic nitrogen-containing ligands. *J. Chem. Soc. Dalton Trans.* **2000**, 3885–3896. [[CrossRef](#)]

37. Ward, M.D. Design of crystalline molecular networks with charge-assisted hydrogen bonds. *Chem. Commun.* **2005**, 5838–5842. [[CrossRef](#)] [[PubMed](#)]
38. Heering, C.; Nateghi, B.; Janiak, C. Charge-Assisted Hydrogen-Bonded Networks of NH_4^+ and $[\text{Co}(\text{NH}_3)_6]^{3+}$ with the New Linker Anion of 4-Phosphono-Biphenyl-4'-Carboxylic Acid. *Crystals* **2016**, *6*, 22. [[CrossRef](#)]
39. Chamayou, A.-C.; Neelakantan, M.A.; Thalamuthu, S.; Janiak, C. The first vitamin B6 zinc complex, pyridoxinato-zinc acetate: A 1D coordination polymer with polar packing through strong inter-chain hydrogen bonding. *Inorg. Chim. Acta* **2011**, *365*, 447–450. [[CrossRef](#)]
40. Drašković, B.M.; Bogdanović, G.A.; Neelakantan, M.A.; Chamayou, A.-C.; Thalamuthu, S.; Avadhut, Y.S.; Schmedt auf der Günne, J.; Banerjee, S.; Janiak, C. N-o-Vanillylidene-L-histidine: Experimental charge density analysis of a double zwitterionic amino acid Schiff-base compound. *Cryst. Growth Des.* **2010**, *10*, 1665–1676. [[CrossRef](#)]
41. Dorn, T.; Chamayou, A.-C.; Janiak, C. Hydrophilic interior between hydrophobic regions in inverse bilayer structures of cation-1,1'-binaphthalene-2,2'-diyl phosphate salts. *New J. Chem.* **2006**, *30*, 156–167. [[CrossRef](#)]
42. Maclaren, J.K.; Sanchiz, J.; Gili, P.; Janiak, C. Hydrophobic-exterior layer structures and magnetic properties of trinuclear copper complexes with chiral amino alcoholate ligands. *New J. Chem.* **2012**, *36*, 1596–1609. [[CrossRef](#)]
43. Naik, A.; Marchand-Brynaert, J.; Garcia, Y. A Simplified Approach to N-and N,N'-Linked 1,2,4-Triazoles by Transamination. *Synthesis* **2008**, *1*, 149–154.
44. Bartlett, R.K.; Humphrey, I.R. Transaminations of NN-dimethylformamide azine. *J. Chem. Soc. C* **1967**, 1664–1666. [[CrossRef](#)]
45. APEX2. *SAINT, Data Reduction and Frame Integration Program for the CCD Area-Detector System, Bruker Analytical X-ray Systems, Data Collection program for the CCD Area-Detector System*; Bruker: Madison, WI, USA, 1997–2006.
46. Sheldrick, G. *SADABS: Area-Detector Absorption Correction*; University of Göttingen: Göttingen, Germany, 1996.
47. Hübschle, C.B.; Sheldrick, G.M.; Dittrich, B. ShelXle: A graphical user interface for SHELXL. *J. Appl. Cryst.* **2011**, *44*, 1281–1284. [[CrossRef](#)] [[PubMed](#)]
48. Brandenburg, K. Crystal and Molecular Structure Visualization, Crystal Impact—K. In *Diamond*; version 3.2; Brandenburg, H., Ed.; Putz Gbr: Bonn, Germany, 2009.
49. Spek, A.L. Structure validation in chemical crystallography. *Acta Crystallogr. Sect. D Biol. Crystallogr.* **2009**, *65*, 148–155. [[CrossRef](#)] [[PubMed](#)]



© 2016 by the authors; licensee MDPI, Basel, Switzerland. This article is an open access article distributed under the terms and conditions of the Creative Commons by Attribution (CC-BY) license (<http://creativecommons.org/licenses/by/4.0/>).